

Combinatory approach of methacrylated alginate and acid monomers for concrete applications

Peer-reviewed author version

Mignon, Arn; DEVISSCHER, Dries; GRAULUS, Geert-Jan; Stubbe, Birgit; Martins, Jose; Dubruel, Peter; De Belie, Nele & Van Vlierberghe, Sandra (2017) Combinatory approach of methacrylated alginate and acid monomers for concrete applications. In: CARBOHYDRATE POLYMERS, 155, p. 448-455.

DOI: 10.1016/j.carbpol.2016.08.102

Handle: <http://hdl.handle.net/1942/22766>

Combinatory approach of methacrylated alginate and acid monomers for concrete applications

Arn Mignon^{a,b}, Dries Devisscher^{b,c}, Geert-Jan Graulus^b, Birgit Stubbe^b, José Martins^d, Peter Dubruel^b, Nele De Belie^{a,*} and Sandra Van Vlierberghe^{b,*}

^a Magne Laboratory for Concrete Research, Department of Structural Engineering, Ghent University, Technologiepark Zwijnaarde 904, B-9052 Ghent, Belgium.

Arn.Mignon@ugent.be, Nele.DeBelie@ugent.be

^b Polymer Chemistry & Biomaterials Research Group, Department of Organic and Macromolecular Chemistry, Ghent University, Krijgslaan 281, Building S4-bis, B-9000 Ghent, Belgium.

Arn.Mignon@ugent.be, Peter.Dubruel@ugent.be, Sandra.VanVlierberghe@ugent.be, Geertjan.Graulus@ugent.be, Birgit.Stubbe@ugent.be

^c Design & Synthesis of Organic Semiconductors, Institute for Materials Research, Hasselt University, Agoralaan 1 – Building D, 3590 Diepenbeek, Belgium

Dries.Devisscher@uhasselt.be

^d NMR and Structure Analysis Unit, Department of Organic Chemistry, Ghent University, Krijgslaan 281, Building S4 bis, B-9000 Ghent, Belgium

Jose.Martins@UGent.be

*Corresponding author: Sandra Van Vlierberghe
Krijgslaan 281, S4-bis
B-9000 Ghent, Belgium
e-mail: Sandra.VanVlierberghe@UGent.be
tel: 003292644508
fax: 003292644998

Abstract:

Polysaccharides, and especially alginate, can be useful for self-healing of cracks in concrete. Instead of weak electrostatic bonds present within calcium alginate, covalent bonds, by methacrylation of the polysaccharides, will result in mechanically stronger superabsorbent polymers (SAPs). These methacrylated alginate chains as backbone are combined with two acrylic monomers in a varying molar fraction. These SAPs show a moisture uptake capacity up to 110% their own weight at a relative humidity of 95%, with a negligible hysteresis. The swelling capacity increased (up to 246 times its own weight) with a decreasing acrylic acid/2 acrylamido-2-methylpropane sulfonic acid ratio. The SAPs also showed a thermal stability up to 200°C. Interestingly, the SAP composed of alginate and acrylic acid exerted a very limited decrease in compressive strength (up to 7% with addition of 1 wt% SAP) rendering this material interesting for the envisaged self-healing application.

Keywords:

polysaccharide; alginate; self-healing; concrete; swelling potential; compressive strength

45
46
47
48
49
50
51
52
53
54
55
56
57
58
59
60
61
62
63
64
65
66
67
68
69
70
71
72
73
74
75
76
77
78
79
80
81
82
83
84
85
86
87
88

1. Introduction

Reports have been presented in literature covering synthetic superabsorbent polymers (SAPs) used in concrete for various applications such as internal curing (Mechtcherine et al., 2014; Viktor Mechtcherine, 2006), frost resistance (Jensen, 2013; Laustsen, Hasholt & Jensen, 2013) and self-sealing and -healing of cracks (Mignon et al., 2014; Snoeck, Van Tittelboom, De Belie, Steuperaert & Dubruel, 2012; Snoeck, Van Tittelboom, Steuperaert, Dubruel & De Belie, 2014). The use of synthetic SAPs has been proven to be promising as a smart internal solution for this latter application (Mignon et al., 2014; Mignon et al., 2015b; Snoeck, Van Tittelboom, Steuperaert, Dubruel & De Belie, 2014). However, these synthetic materials often compromise the material strength, which is undesired in the construction industry. On the one hand, the SAP particles will cause internal curing by releasing their entrained mixing water, stimulating the densification and further hydration of the cementitious matrix and reducing autogenous shrinkage and hence, the risk at early age cracking. These consequences can lead to an increase of the overall material strength. Conversely, after the release of the entrained water by the SAPs, air-filled macropores will remain present in the matrix, which generally leads to a decrease of the overall concrete strength (Hasholt, Jensen, Kovler & Zhutovsky, 2012; Laustsen, Hasholt & Jensen, 2013; Snoeck, Schaubroeck, Dubruel & De Belie, 2014). As for self-sealing (Snoeck, Steuperaert, Van Tittelboom, Dubruel & De Belie, 2012) and self-healing applications (Snoeck, Schaubroeck, Dubruel & De Belie, 2014; Snoeck, Van Tittelboom, Steuperaert, Dubruel & De Belie, 2014) high SAP amounts are required (up to 1 % relative to cement mass), this macropore formation becomes more critical especially when high amounts of additional water are used to compensate for the loss in workability. Previous research has proven that polysaccharides and especially alginate, are very promising as starting materials for self-sealing and -healing of cracks. However, instead of the weak electrostatic bonds present within calcium alginate which are prone to disintegration in the presence of monovalent cations (Bajpai & Sharma, 2004), covalent linkages generally result in mechanically superior SAPs (Povh & Rosina, 2005). One way to create covalent bonds in a SAP network based on polysaccharides is by first modifying them with methacrylic anhydride (MAAH) (Chou, Akintoye & Nicoll, 2009; Chou & Nicoll, 2009). MAAH can be used to enable cross-linking of the polysaccharides. In the case of alginate, the hydroxyl groups will react with the anhydride resulting in methacrylated alginate. These methacrylate functions can be used to execute a free radical polymerization in the presence of acrylic monomers.

Acrylic acid (AA) has already been proven to be a widespread used monomer for the development of synthetic SAPs, often in combination with other acrylic monomers such as acrylamide (Ding, Xiao, An & Jia, 2006; Mohammad J. Zohuriaan-Mehr 2008; Nesrinne & Djamel, 2013; Zhang, Cui, Yin, Li, Liao & Cai, 2011; Zhou et al., 2003). Another interesting monomer is 2-acrylamido-2-methylpropanesulfonic acid (AMPS) as this hydrophilic, sulfonic acid possesses a large swelling capacity and has already been used in a variety of applications going from water treatment (Kang & Cao, 2012; Yu et al., 2011) and drug delivery (Pourjavadi, Barzegar & Zeidabadi, 2007) towards other biomedical applications (Anirudhan & Sandeep, 2011; Keogh, 1995; Keogh, Hobot, Eaton, Jevne & Bergan, 1995) and personal care (Abdel-Azim, Farahat, Atta & Abdel-Fattah, 1998; Cahalan & Coury, 1986; Lundmark, Melby & Chun, 1978).

89 The present manuscript reports on the development and characterization of SAPs based on
90 methacrylated alginate as backbone combined with a varying molar fraction of a carboxylic acid (AA)
91 and/or a sulfonic acid (AMPS). The degree of methacrylation after modification will be determined by
92 proton nuclear magnetic resonance spectroscopy. After polymerization, the gel fraction and particle
93 size distribution will be identified. The chemical structure of the synthesized SAPs will be verified
94 through attenuated total reflectance-infrared (ATR-IR) spectroscopy. High resolution magic-angle
95 spinning (HR-MAS) ¹H-NMR spectroscopy will be used to identify the polymerization efficiency. In
96 addition, the sorption and desorption of moisture at different relative humidities will be measured by
97 dynamic vapor sorption (DVS) measurements. It is also important to identify the swelling degree in
98 aqueous (ultrapure water and demineralized water) and cement filtrate solutions. Additionally, the
99 thermal stability is evaluated using thermogravimetric analysis (TGA). Finally, the influence of these
100 SAPs on the strength of mortar is also determined.

101

102 2. Materials and methods

103

104 2.1. Materials

105

106 2-Acrylamido-2-methylpropane sulfonic acid (AMPS), ammonium persulfate (APS), sodium alginate
107 (NaAlg, M/G ratio of 2.3, Mw of 76 kDa and a \bar{D} of 4.6) and methacrylic anhydride (MAAH) have been
108 bought from Sigma-Aldrich (Bornem, Belgium). Acrylic acid (AA) and N,N,N',N'- tetramethylethylene-
109 diamine (TEMED) originated from Acros Organics (Geel, Belgium). N,N'-methylene bisacrylamide
110 (MBA) came from Merck (Nottingham, UK). The paper filters (retention of 8 – 12 μ m) were
111 purchased at Munktell filters (Bärenstein, Germany).

112

113 2.2. Modification of alginate backbone with methacrylate moieties

114

115 A derivatization of alginate with methacrylic anhydride (MAAH), based on a reaction of the hydroxyl
116 moieties of the polysaccharide backbone with the anhydride, was carried out to incorporate
117 methacrylate groups for network formation. A 2 wt% sodium alginate solution was prepared in
118 demineralized water using a mechanical stirrer. Subsequently, MAAH was added dropwise to the
119 solution. The added amount corresponded with 2 equivalents of MAAH with respect to the hydroxyl
120 groups from alginate. During the reaction, methacrylic acid was released which lowers the pH of the
121 reaction. However, the acidity of the mixture was constantly monitored and the pH was increased to
122 8 by adding small amounts of a 5 M sodium hydroxide (NaOH) solution. Conversely, the pH should
123 not be too high to avoid hydrolysis of the ester in the reaction product. The mixture was reacted at
124 room temperature for 24 hours after the addition of MAAH. Afterwards, dialysis (12 – 14 kDa) was
125 performed for 72 hours while changing the dialysis water twice a day to remove unreacted agents
126 and formed methacrylic acid. The resulting solution afforded modified alginate (algMOD) by
127 lyophilization.

128

129 2.3. Detailed characterization of the synthesized SAPs

130

131 After polymerization, unreacted particles were removed from the end product via dialysis. By
132 measuring the dry weight of the sample before and after purification during 24 hours, the gel
133 fraction could be determined using the following equation:

134
$$G [\%] = W/W_0 \quad (1)$$

135 W = mass of the dry insoluble part of the sample

136 W_0 = initial dry mass of the sample

137

138 To examine the resulting particle size diameters of all grinded materials (grinded with an A11 basic
139 Analytical Mill), a Zeiss Axiotech optical microscope was used together with the digital image
140 capturing software ZEN core and the analysing software ImageJ. A sample population > 100 has been
141 used. The statistical analysis was performed by creating a size distribution curve.

142

143 The SAP powder was subsequently characterized using attenuated total reflectance infrared (ATR-IR)
144 spectroscopy. A BioRad FTS 575C combined with a MKII Golden Gate setup equipped with a diamond
145 crystal from Specac was used for all experiments. These results were analysed with the Bio-Rad Win-
146 IR Pro software.

147

148 The ^1H -NMR spectra were obtained by dissolving the samples in D_2O (10 mg/ml) and recording the
149 samples at room temperature on a Varian Inova 400 MHz spectrometer using a 5 mm four-nucleus
150 PFG probe with water suppression.

151

152 High Resolution Magic-Angle Spinning NMR (HR-MAS ^1H -NMR) spectroscopy analysis of the
153 developed SAPs was performed on a Bruker Avance II 700 spectrometer (700.13 MHz) using a HR-
154 MAS probe equipped with a ^1H , ^{13}C , ^{119}Sn and gradient channel. The spinning rate was set to 6 kHz.
155 Samples were prepared by placing a small amount of freeze-dried material inside a 4 mm zirconium
156 oxide MAS rotor (80 μL). 30 μL D_2O was added to the rotor, allowing the samples to swell. The
157 samples were homogenized by manual stirring prior to analysis. A teflon[®] coated cap was used to
158 close the rotor.

159

160 Dynamic vapor sorption (DVS) experiments were applied as described earlier in (Mignon et al.,
161 2015a) with systematic steps of 20, 40, 60, 80, 90 and 95% RH.

162

163 Swelling tests performed in ultrapure and demineralized water

164 The swelling capacity of the SAPs was determined as the mass change between the freeze-dried and
165 the swollen (cfr. saturated) state. A mass of 0.15 - 0.20 g polymer was incubated in 100 mL of
166 aqueous solution. After 3h incubation, a funnel and a filter were used to capture the water that was
167 not absorbed by the SAPs. By calculating the difference between the initially added and the filtered
168 water, the residual water inside the material could be determined together with the swelling
169 capacity of the material using Equation (5):

170

171
$$\text{Swelling capacity} = (m_0 - m_{\text{filter}}) / m_{\text{SAP}} \quad (5)$$

172 where m_0 is the initially added water mass [g], m_{filter} represents the mass of the water going through
173 the filter [g] and m_{SAP} is the added mass of dried SAP (i.e. 0.20 g). The filtration paper was typically
174 saturated prior to the filtration to exclude its influence on the mass of the filtered water.

175

176 Swelling tests in cement filtrate solutions

177 Cement filtrate (CF) was made by mixing 10 g ordinary Portland cement (OPC) and 100 mL
178 demineralized water for three hours with a mechanical stirrer, followed by filtration to remove the
179 cement particles and collecting the solution. The same conditions as for aqueous solutions were used
180 for further analysis. All swelling tests were performed in triplicate.

181
182 The thermal properties were analyzed using thermogravimetric analysis (TGA) using a TA-
183 instruments Q-50 Thermogravimetric Analyzer as described earlier in (Mignon et al., 2015b) with a
184 maximal temperature of 600°C and a starting equilibrium temperature of 30°C.

185 2.4. Bending and compression strength measurements

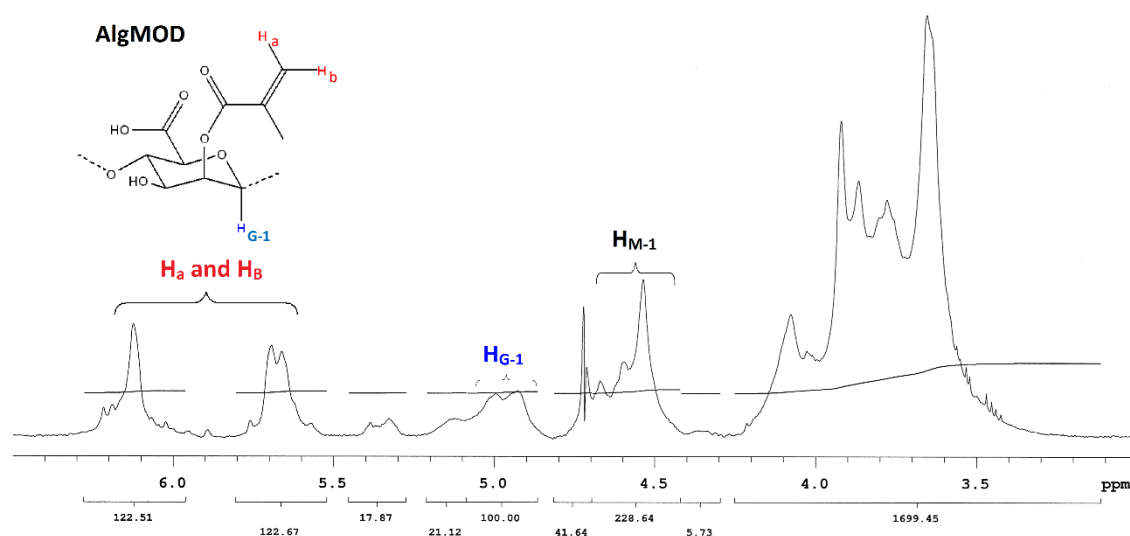
186
187
188 Mortar samples were manufactured by a standard mortar mixing procedure, as described in detail in
189 EN 196-1 to investigate the influence of the addition of SAPs on the flexural and compression
190 strength of mortar samples. Flexural and compressive strength were measured at the age of 28 days
191 by means of a three-point-bending test followed by a compression test on the resulting halves
192 following the Standard NBN EN 196-1 and described in detail in (Mignon et al., 2015b).

193 194 195 3. Results and discussion

196 197 3.1. Methacrylation of alginate through modification with methacrylic anhydride

198
199 In a first step, alginate was methacrylated yielding algMOD. The degree of methacrylation (DM, or
200 the degree of substitution, DS) (i.e. the amount of double bonds incorporated on alginate) has a
201 strong influence on the physical properties as well as the swelling capacity of the formed SAP. For
202 that reason, it is important to calculate the DS using ^1H NMR spectroscopy (as described in section
203 2.6).

204



205
206 Figure 1: ^1H NMR spectrum of algMOD with annotation of the relevant peaks for the calculation of
207 the DS (H_a and H_b as protons connected to the $\text{C}=\text{C}$ bond, a proton on the α -l-guluronic acid structure
208 (H_{G-1}), and a reference proton on the β -d-mannuronic acid (H_{M-1} , not shown on molecular structure).

209

210 The obtained spectra were analyzed by comparing the characteristic peaks of the methacrylate
 211 moieties corresponding to the vinyl protons at 5.73 and 6.16 ppm with the reference peak from the
 212 alginate backbone at 4.97 ppm. As the latter corresponds with the anomeric carbon of the guluronic
 213 acid block (G-units), the G-value had to be calculated and incorporated as a correction factor due to
 214 the presence of mannuronic acid (M-units). Therefore, the relative proportion of the G-units
 215 compared to the total amount of G- and M-units had to be determined by using Equation 2.
 216 Subsequently, the average of the peaks of the methacrylate groups was calculated and used to
 217 compute the degree of substitution (DS) per repeating unit by applying Equation 3. To obtain the DS
 218 with respect to the hydroxyl groups, this value had to be divided by two as the considered repeating
 219 unit (G-unit) possessed two hydroxyl groups.

220

$$221 \quad G [\%] = \frac{H_{G-1}}{H_{M-1}+H_{G-1}} = \frac{I_{4.97ppm}}{I_{4.58ppm}+I_{4.97ppm}} * 100\% \quad (2)$$

222

$$223 \quad DS [\%] = G * \frac{H_a+H_b}{H_{G-1}} = G * \frac{I_{5.73ppm}+I_{6.16ppm}}{I_{4.97ppm}} \quad (3)$$

224

225 The protons H_{G-1} , H_{M-1} , H_a and H_b are related to the intensity of their related peaks on the NMR
 226 spectrum, seen further in Figure 1. Using Equations 2 and 3, a relative concentration of
 227 guluronic acid units or G-content of 30.5% and a DS of 18.7% as a function of the present
 228 hydroxyl groups were determined. The latter implies that almost one out of five functional
 229 hydroxyl groups or one of every three repeating units (37.4%) have been modified.

230

231 3.2. SAP development and characterization

232

233 After modification, methacrylated alginate (algMOD) was combined with the monomers (AA and
 234 AMPS) to create a cross-linked network through free radical polymerization. AMPS was selected as
 235 second monomer to compare the effect of a carboxylic acid versus the incorporation of a sulfonic
 236 acid with respect to the swelling capacity as well as the influence on the mortar strength. AlgMOD
 237 combined with AA forms a strong and transparent solid gel while a decrease in AA/AMPS ratio leads
 238 to a more brittle gel. The composition and nomenclature of the SAPs is given in Table 1.

239

240 Table 1: Overview of theoretical chemical composition of the developed SAPs and the gel fraction.

241

The algMOD fraction was added in addition to the total monomer amount.

Sample	<i>AlgMOD</i> AA + AMPS g/g	AA mol%	AMPS mol%	Gel fraction (%)
p(alg(1)_AA ₁₀₀ /AMPS ₀ (7))	1/7	100	0	85.3 ± 1.2
p(alg(1)_AA ₇₅ /AMPS ₂₅ (7))	1/7	75	25	80.9 ± 2.6
p(alg(1)_AA ₅₀ /AMPS ₅₀ (7))	1/7	50	50	61.3 ± 2.2
p(alg(1)_AA ₂₅ /AMPS ₇₅ (7))	1/7	25	75	58.9 ± 1.3
p(alg(1)_AA ₀ /AMPS ₁₀₀ (7))	1/7	0	100	42.7 ± 6.2

242

243 Table 1 also shows that a lower AA/AMPS ratio leads to a significant decrease in the gel fraction. On
 244 the one hand, the materials containing more AMPS were more brittle and thus more prone to
 245 become damaged during purification. In addition, the higher polarity of AMPS could have resulted in
 246 an increased repulsion between negatively charged carboxylate groups on the alginate backbone and
 247 sulfate moieties on the AMPS monomer, thereby hindering the crosslinking reaction.

248
 249 Smaller particles have a higher surface area which can have an influence on a.o. the moisture uptake
 250 capacity. In addition, upon incorporation in mortar, these smaller particles will lead to more smaller
 251 pores compared to larger SAPs. All materials showed a similar particle size for d_{10} and d_{50} (see Table
 252 2). In the table, d_x indicates the diameter where x percentage of the particles is smaller or equal to.
 253 Approximately half of the particles were characterized by a diameter of 20 μm or lower. However,
 254 the d_{90} values show that there was a small variation between the SAPs, which can be related to the
 255 duration of the grinding. However, the difference was quite limited and all diameters ranged
 256 between 50 – 80 μm .

257
 258 Table 2: Particle size ranges of the algMOD - AA/AMPS SAPs where d_{10} , d_{50} and d_{90} indicate the
 259 percentage of particles (10%, 50% and 90%) with a diameter smaller or equal to x μm .

Material	d_{10} [μm]	d_{50} [μm]	d_{90} [μm]
p(alg(1)_AA ₁₀₀ /AMPS ₀ (7))	9-10	20-21	80
p(alg(1)_AA ₇₅ /AMPS ₂₅ (7))	8-9	20-21	47-48
p(alg(1)_AA ₅₀ /AMPS ₅₀ (7))	8-9	18-19	48-49
p(alg(1)_AA ₂₅ /AMPS ₇₅ (7))	10-11	21-22	75-76
p(alg(1)_AA ₀ /AMPS ₁₀₀ (7))	10-11	20-21	67-68

260
 261

262 3.3. Chemical structure confirmation and cross-linking efficiency assessment

263
 264 ATR-IR spectroscopy has been performed on the p(alg_AA/AMPS) SAPs (see Figure 2). The S=O
 265 stretch at 1040 cm^{-1} of the sulfonic acid ((a) in Figure 2), the N-H stretch of the secondary amides
 266 between 3500 and 3100 cm^{-1} and at 1550 cm^{-1} (b) and the C=O stretch of the amides at 1650 cm^{-1} (c)
 267 are clearly stronger present with an increasing amount of AMPS.

268 The C=O stretch of the acid moiety at 1700 cm^{-1} (d) is on the other hand strong for
 269 p(alg(1)_AA₁₀₀/AMPS₀(7)) due to the high amount of AA. These peaks are found by comparing to
 270 earlier performed research (Athawale & Lele, 1998; Athawale & Lele, 2000; Najjar, Yunus, Ahmad &
 271 Rahman, 2000; Rosa, Bordado & Casquilho, 2003).

272 These results give a qualitative indication of the presence of the polysaccharide and the monomers
 273 as well as an increase or decrease of the intensity of certain peaks which is related to the variation of
 274 the AA/AMPS ratio.

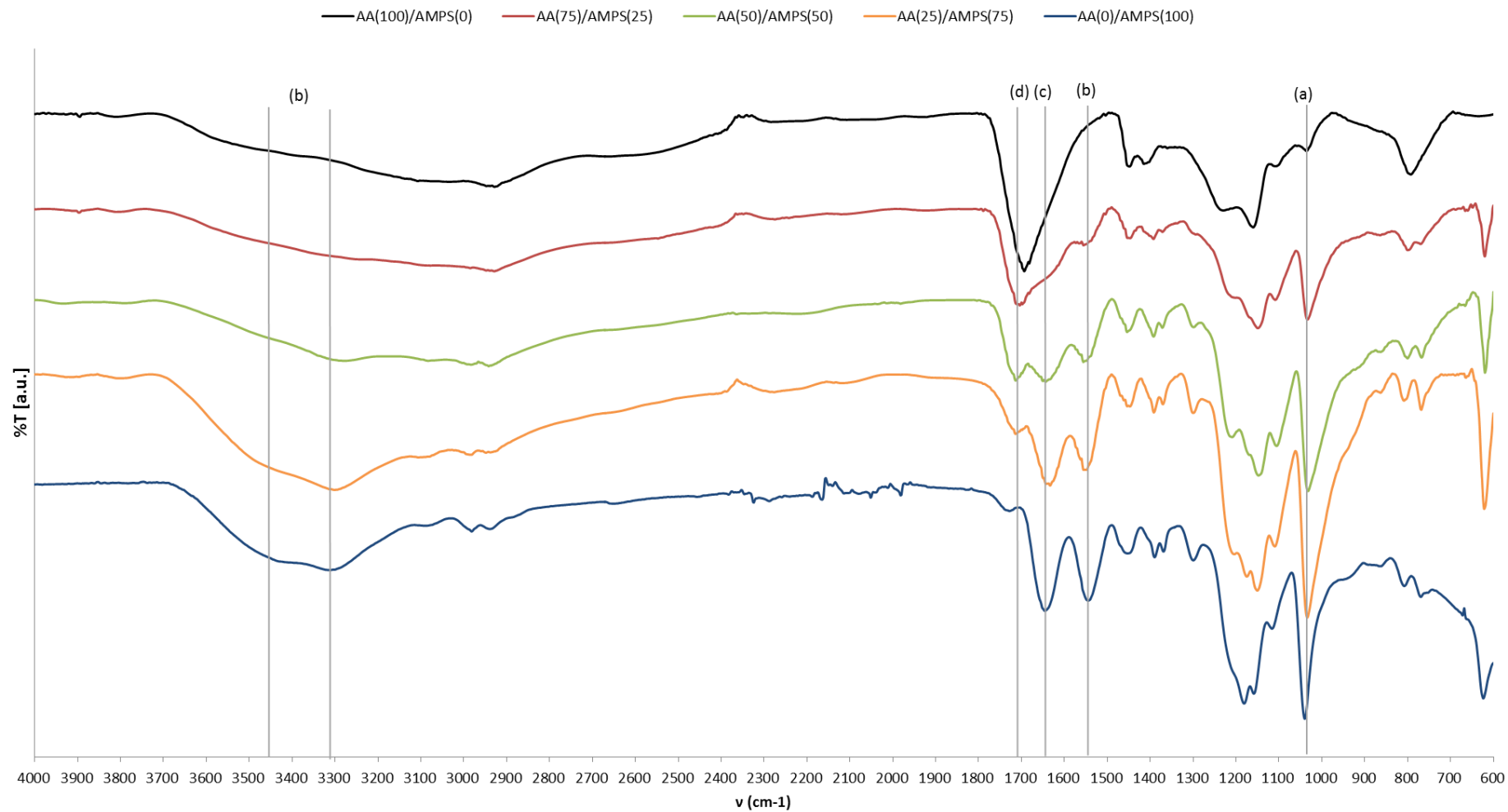
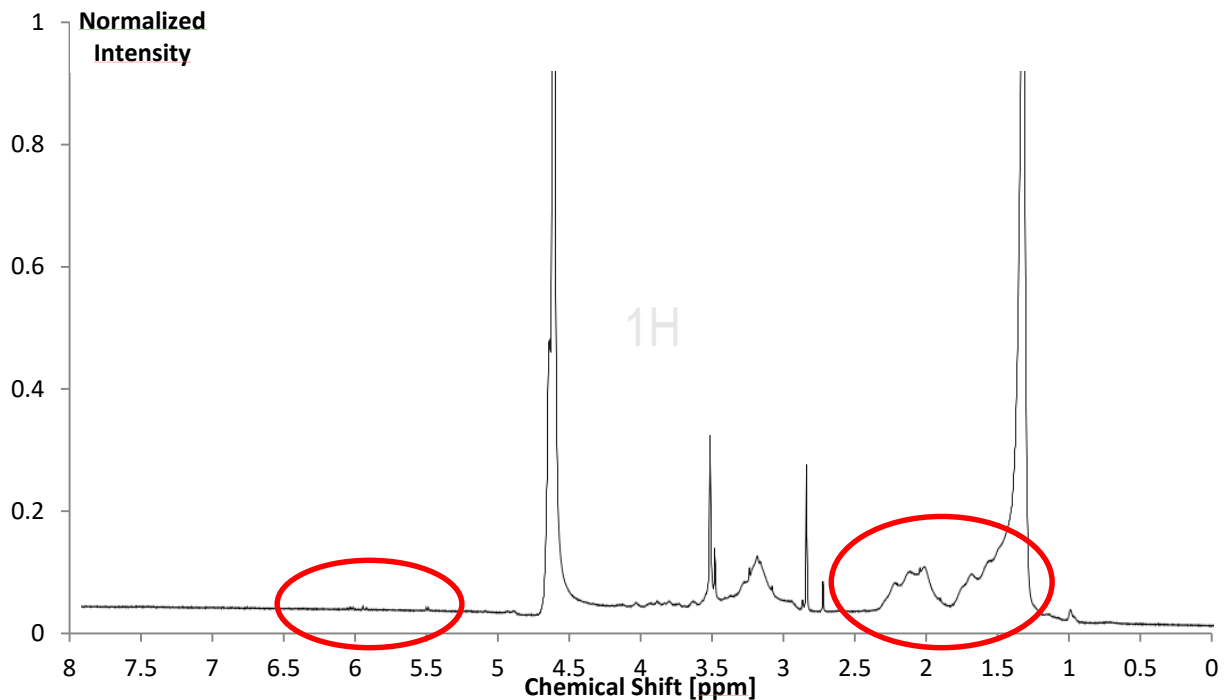


Figure 2: FTIR spectra of the algMOD - AA/AMPS SAPs with annotation of the most relevant peaks. The samples are abbreviated by the molar ratio of the incorporated monomers according to: AA(x) /AMPS(y).

1 HR-MAS ^1H -NMR spectroscopy was used as a technique to confirm the polymerization (cross-linking)
2 efficiency. The peaks corresponding to protons from the C=C double bonds from either the
3 methacrylate functionalities introduced in algMOD or from the monomers are apparent in the range
4 of 5.5 – 6.5 ppm (as indicated in Figure 1 for algMOD). After polymerization, these signals have
5 completely disappeared, as shown in Figure 3 (i.e. p(alg(1)_AA₅₀/AMPS₅₀(7)) as an example). These
6 peaks have shifted to the right (1.5 – 2.5 ppm) by conversion of the double bond protons into alkane
7 protons, adjacent to an electronegative group.
8



9
10 Figure 3: HR-MAS ^1H NMR spectrum of p(alg(1)_AA₅₀/AMPS₅₀(7)). The absence of peaks
11 corresponding to double bond protons (situated between 5.5 and 6.5 ppm) from either algMOD, AA
12 or AMPS confirms the success of the cross-linking reaction.

13 3.4. Determination of the moisture uptake capacity of the SAPs via dynamic vapor sorption

14
15 The moisture uptake capacity of the SAPs has been assessed to identify their behavior in mortar or
16 concrete, when no direct ingress of water or rain is possible upon crack formation. If these SAPs can
17 significantly absorb moisture in humid environments, the cracks may be partially sealed. The results
18 (see Figure 4 (a)) show that with a decrease of the AA/AMPS ratio, the moisture uptake capacity
19 increases, especially at high relative humidity (RH). The values range between 53.6 and 109.8% at a
20 RH of 95%. Materials with ≥ 50 mol% AMPS can even take up more than their original weight in
21 moisture at a RH of 95%. In addition, these materials show a negligible degree of hysteresis. As a
22 result, all moisture taken up can also be completely desorbed again. Indeed, concrete constructions
23 that are not exposed to humid environments can thus still retain a certain amount of moisture from
24 air at the crack faces. In a subsequent stage, the SAPs are likely to completely deliver this moisture to
25 remaining unreacted cement particles, which can lead to formation of new cement hydration
26 products and deposition of CaCO_3 from dissolved $\text{Ca}(\text{OH})_2$ and CO_2 , thereby contributing to the
27 development of self-healing applications (Snoeck, Van Tittelboom, Steuperaert, Dubruel & De Belie,
28 2014).
29

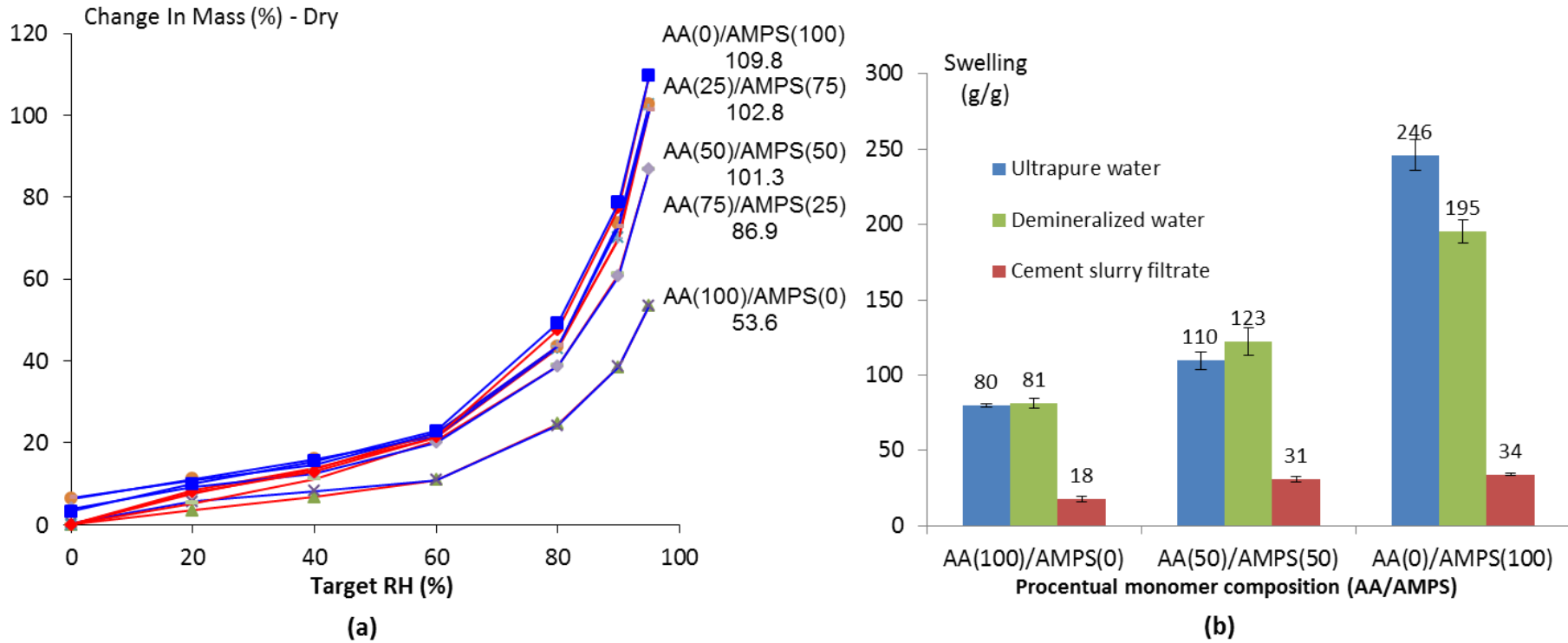
30 The reason for the higher moisture uptake capacity upon decreasing the AA/AMPS ratio can be
31 attributed to the higher polarity of the sulfonic acid compared to the carboxylic acid. On the other
32 hand, the increase can also be related to the higher amount of sulfonic acid groups being ionized at
33 the same pH. Although this effect will be rather limited for DVS measurements, it will clearly be more
34 pronounced in the swelling capacity.

35

36 3.5. Swelling capacity measurements on the synthesized SAPs

37

38 The swelling potential of the SAPs was determined in three swelling media (i.e. ultrapure water,
39 demineralized water and cement filtrate solution). As such, a difference in the ionic concentration
40 will result in a variation of the swelling capacity. On the other hand, the monomer ratio (AA/AMPS)
41 will also have a strong influence on the swelling degree. Therefore, three samples with varying
42 monomer ratio were selected for further testing including p(alg(1)_AA₁₀₀/AMPS₀(7)),
43 p(alg(1)_AA₅₀/AMPS₅₀(7)) and p(alg(1)_AA₀/AMPS₁₀₀(7)). The results show (see Figure 4 (b)) that the
44 swelling potential in cement filtrate is significantly ($p < 0.05$) lower, as anticipated due to the
45 presence of Ca^{2+} , Mg^{2+} and other ions (Mignon et al., 2015b) as well as the lower osmotic pressure in
46 a solution with a high ion concentration (Horkay, Tasaki & Basser, 2000). No significant differences
47 could be observed between ultrapure water and demineralized water except for
48 p(alg(1)_AA₀/AMPS₁₀₀(7)). Due to the high swelling of the latter, the relatively higher ion
49 concentration of demineralized water resulted in a swelling reduction. An observed trend for the
50 AA/AMPS ratio is that for all solutions, a decrease of the ratio leads to an increase of the swelling
51 capacity, which is in excellent agreement with the obtained DVS results.



52

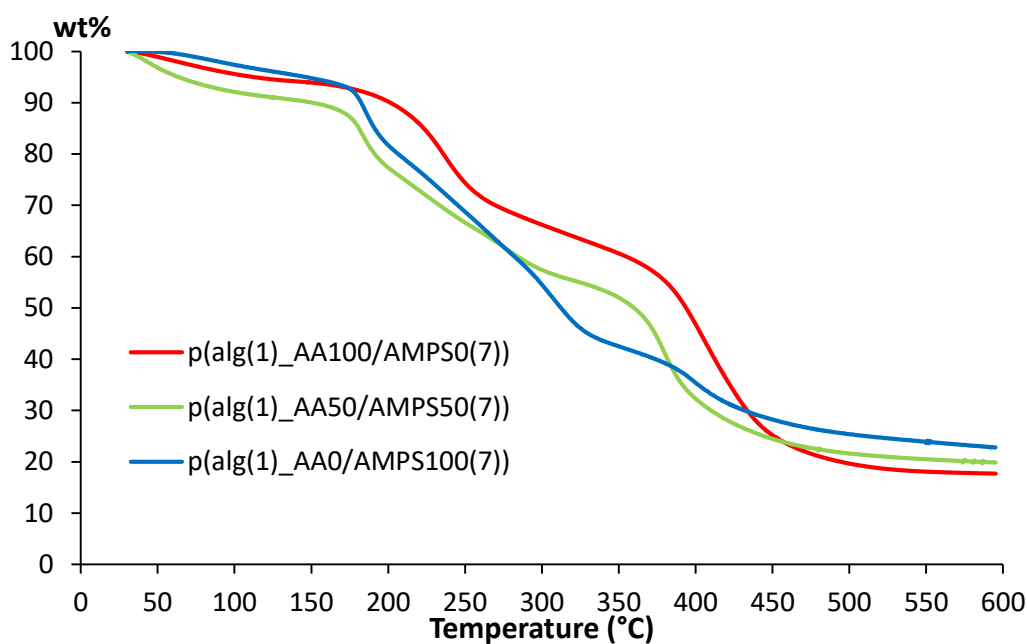
53 Figure 4: **(a)** Sorption and desorption isotherms of p(algMOD_AA/AMPS) materials measured by a Dynamic Vapor Sorption apparatus. The values
 54 underneed the sample names describe the maximal moisture uptake capacity (at 95% RH). **(b)** Swelling potential of the synthesized SAPs in ultrapure water,
 55 demineralized water and cement filtrate solution with a pH of 12.6. The samples are abbreviated by the molar ratio of the incorporated monomers
 56 according to: AA(x)/AMPS(y).

57

58 3.6. Thermal stability of the SAPs assessed by thermogravimetric analysis

59

60 The production of the SAPs occurs at 45°C while the temperature of concrete can rise up to 50 - 60°C
61 during curing (Snoeck, 2015). Ideally, the polymers should not show thermal degradation at these
62 temperatures. In order to study potential thermally induced degradation, TGA measurements were
63 performed (see Figure 5). The results showed that at 100°C, over 90% of the material was
64 maintained, while this loss can be attributed to residual water being present in the SAP as they were
65 kept in the lab and no freeze drying step was performed right before the TGA measurements.
66 Subsequently, the step at 200 – 250°C can be related to either the decarboxylation of the polymer
67 and when AMPS is present the decomposition of sulfate groups. The last step around 360 – 450°C is
68 the main chain C-C fission (Abdelaal, Makki & Sobahi, 2012; Diao et al., 2010).



69

70 Figure 5: TGA plots displayed as the percentual weight as a function of temperature for
71 p(alg(1)_AA₁₀₀/AMPS₀(7)), p(alg(1)_AA₅₀/AMPS₅₀(7)) and p(alg(1)_AA₀/AMPS₁₀₀(7)).

72

73 3.7. Effect of SAPs on the flexural and compressive strength of mortar samples

74

75 As the envisaged application includes their use in concrete, the SAPs were incorporated in mortar to
76 investigate their effect on the flexural and compressive strength of the mortar samples. The
77 composition of the mortar mixture is described in the materials and methods (chapter 2.11.)

78 Ideally, the SAPs should only exhibit a limited or no influence on the strength upon incorporating
79 them in mortar. Interestingly (Table 3), p(alg(1)_AA₁₀₀/AMPS₀(7)) only results in a limited
80 compressive strength reduction up to 7% upon addition of 1 wt% compared to the added amount of
81 cement. This material can thus be considered extremely promising. The data indicate that SAPs with
82 a higher molar fraction of AMPS lead to severely weaker mortar compared to the reference for both
83 the bending and compressive strength, up to the point that they are not useful anymore for the
84 envisaged application. Upon addition of 1 wt% p(alg(1)_AA₀/AMPS₁₀₀(7)) with respect to the added
85 amount of cement, the matrix collapsed and was too weak to assess bending and compressive
86 strength.

87 Table 3: Information on the additional water added on top of the 225g water initially, as well as the
 88 results of the three point bending and compression tests performed on the mortar samples
 89 containing 0.5 or 1 wt% p(alg(1)_AA_x/AMPS_y(7)).

Sample description	SAP concentration [w%]	Additional water [ml]	Bending strength [MPa]	Compressive strength [MPa]
Reference	0	0	7.6 ± 0.5	73.1 ± 1.6
p(alg(1)_AA ₁₀₀ /AMPS ₀ (7))	0.5	15	6.8 ± 0.4 (-11%)	68.9 ± 1.6 (-6%)
	1	30	7.6 ± 0.3 (/)	68.3 ± 0.6 (-7%)
p(alg(1)_AA ₅₀ /AM ₅₀ (7))	0.5	80	6.3 ± 0.4 (-17%)	42.1 ± 1.4 (-42%)
	1	150	5.1 ± 0.6 (-33%)	26.9 ± 0.2 (-63%)
p(alg(1)_AA ₀ /AMPS ₁₀₀ (7))	0.5	100	5.9 ± 0.3 (-22%)	36.6 ± 0.9 (-50%)

90

91 4. Conclusions and future perspectives

92

93 Alginate was successfully modified using methacrylic anhydride to create methacrylated alginate
 94 (algMOD) with a DS of 19% with respect to the hydroxyl groups present. ATR-IR and HR-MAS ¹H-NMR
 95 spectroscopy enabled to confirm the SAP structure as well as the cross-linking efficiency. The
 96 materials possessed gel fractions ranging between 43 and 85%, which decreased upon decreasing
 97 the AA/AMPS molar ratio. The SAPs showed a moisture uptake capacity going from 54 to 110% their
 98 own weight at a RH of 95% upon increasing the AMPS ratio. Interestingly, all materials showed a
 99 negligible hysteresis which implies that they can be used as a reservoir and all moisture taken up will
 100 also be completely desorbed again. When investigating the swelling capacity, it was observed that an
 101 increase of the AMPS content led to an increased swelling, independent of the used solution, up to a
 102 maximal swelling potential of 246 times its own weight for p(alg(1)_AA₀/AMPS₁₀₀(7)) in ultrapure
 103 water. Additionally, these polymers showed a thermal stability above 100°C, indicating that they will
 104 not degrade during the curing of the concrete matrix. After incorporation of the SAPs in mortar, it
 105 was determined that a decrease of the AA/AMPS ratio resulted in a severe decrease of the
 106 compressive strength of mortar. Interestingly, p(alg(1)_AA₁₀₀/AMPS₀(7)) showed only a very limited
 107 decrease in compressive strength (up to 7% decrease upon addition of 1 wt% SAP). Despite the
 108 rather limited moisture uptake and swelling capacity, this latter material showed the highest gel
 109 fractions and very limited effect on the compressive strength, rendering this material very interesting
 110 for the envisaged application. This material will thus be further tested for its self-sealing and -healing
 111 potential. The latter will be the topic of a forthcoming paper.

112

113 **Acknowledgement**

114

115 The authors would like to thank the FWO (Research Foundation Flanders) for project funding
 116 (3G019012, Effect of tunable hydrogels on concrete microstructure, moisture properties, sealing and
 117 self-healing of cracks). The authors would like to acknowledge the group of Peter Adriaensens and
 118 especially Gunter Reekmans for the calculation of the degree of methacrylation of algMOD (Organic
 119 and Bio-polymer Chemistry Department, UHasselt).

120

121 **References:**

- 122 Abdel-Azim, A. A. A., Farahat, M. S., Atta, A. M., & Abdel-Fattah, A. A. (1998). Preparation and
123 properties of two-component hydrogels based on 2-acrylamido-2-methylpropane sulphonic acid.
124 *Polymers for Advanced Technologies*, 9(5), 282-289.
- 125 Abdelaal, M. Y., Makki, M. S. I., & Sobahi, T. R. A. (2012). Modification and characterization of
126 polyacrylic acid for metal ion recovery. *American Journal of Polymer Science*, 2(4), 73-78.
- 127 Anirudhan, T. S., & Sandeep, S. (2011). Synthesis and characterization of molecularly imprinted
128 polymer of N-maleoylchitosan-grafted-2-acrylamido-2-methylpropanesulfonic acid and its controlled
129 delivery and recognition of bovine serum albumin. *Polymer Chemistry*, 2(9), 2052-2061.
- 130 Bajpai, S. K., & Sharma, S. (2004). Investigation of swelling/degradation behaviour of alginate beads
131 crosslinked with Ca²⁺ and Ba²⁺ ions. *Reactive and Functional Polymers*, 59(2), 129-140.
- 132 Cahalan, P. T., & Coury, A. J. (1986). Method of preparing tape electrode. Google Patents.
- 133 Chou, A. I., Akintoye, S. O., & Nicoll, S. B. (2009). Photo-crosslinked alginate hydrogels support
134 enhanced matrix accumulation by nucleus pulposus cells in vivo. *Osteoarthritis and Cartilage*, 17(10),
135 1377-1384.
- 136 Chou, A. I., & Nicoll, S. B. (2009). Characterization of photocrosslinked alginate hydrogels for nucleus
137 pulposus cell encapsulation. *Journal of Biomedical Materials Research Part A*, 91(1), 187-194.
- 138 Diao, H., Yan, F., Qiu, L., Lu, J., Lu, X., Lin, B., Li, Q., Shang, S., Liu, W., & Liu, J. (2010). High
139 Performance Cross-Linked Poly(2-acrylamido-2-methylpropanesulfonic acid)-Based Proton Exchange
140 Membranes for Fuel Cells. *Macromolecules*, 43(15), 6398-6405.
- 141 Ding, Y., Xiao, C., An, S., & Jia, G. (2006). Water-absorptive blend fibers of copoly(acrylic acid-
142 acrylamide) and poly(vinyl alcohol). *Journal of Applied Polymer Science*, 100(4), 3353-3357.
- 143 Hasholt, M. T., Jensen, O. M., Kovler, K., & Zhutovsky, S. (2012). Can superabsorbent polymers
144 mitigate autogenous shrinkage of internally cured concrete without compromising the strength?
145 *Construction and Building Materials*, 31, 226-230.
- 146 Horkay, F., Tasaki, I., & Basser, P. J. (2000). Osmotic swelling of polyacrylate hydrogels in
147 physiological salt solutions. *Biomacromolecules*, 1(1), 84-90.
- 148 Jensen, O. M. (2013). Use of superabsorbent polymers in concrete. *Concrete International*, 35(1), 48-
149 52.
- 150 Kang, G.-d., & Cao, Y.-m. (2012). Development of antifouling reverse osmosis membranes for water
151 treatment: a review. *Water research*, 46(3), 584-600.
- 152 Keogh, J. R. (1995). Contacting blood with medical equipment having polymerized 2-acrylamido-2-
153 methylpropanesulfonic acid on exposed surface. Google Patents.
- 154 Keogh, J. R., Hobot, C. M., Eaton, J. W., Jevne, A. H., & Bergan, M. A. (1995). Made from monomers
155 such as N-(3-aminopropyl) methacrylamide hydrochloride, 2-acrylamido-2-methylpropanesulfonic
156 acid, acrylamide and acrylic acid bonded to polymeric substrate surface; useful in medical devices.
157 Google Patents.
- 158 Laustsen, S., Hasholt, M., & Jensen, O. (2013). Void structure of concrete with superabsorbent
159 polymers and its relation to frost resistance of concrete. *Materials and Structures*, 48(1-2), 357-368.
- 160 Lundmark, L. D., Melby, A., & Chun, H.-m. (1978). Method of imparting lubricity to keratinous
161 substrates and mucous membranes. Google Patents.
- 162 Mechtcherine, V., Gorges, M., Schroefl, C., Assmann, A., Brameshuber, W., Ribeiro, A., Cusson, D.,
163 Custódio, J., da Silva, E., Ichimiya, K., Igarashi, S.-i., Klemm, A., Kovler, K., de Mendonça Lopes, A.,
164 Lura, P., Nguyen, V., Reinhardt, H.-W., Filho, R., Weiss, J., Wyrzykowski, M., Ye, G., & Zhutovsky, S.
165 (2014). Effect of internal curing by using superabsorbent polymers (SAP) on autogenous shrinkage
166 and other properties of a high-performance fine-grained concrete: results of a RILEM round-robin
167 test. *Materials and Structures*, 47(3), 541-562.
- 168 Mignon, A., Graulus, G.-J., Snoeck, D., Martins, J., De Belie, N., Dubruel, P., & Van Vlierberghe, S.
169 (2014). pH-sensitive superabsorbent polymers: a potential candidate material for self-healing
170 concrete. *Journal of Materials Science*, 50(2), 970-979.

171 Mignon, A., Graulus, G.-J., Snoeck, D., Martins, J., De Belie, N., Dubruel, P., & Van Vlierberghe, S.
172 (2015a). pH-sensitive superabsorbent polymers: a potential candidate material for self-healing
173 concrete. *Journal of Materials Science*, 50(2), 970-979.

174 Mignon, A., Snoeck, D., Schaubroeck, D., Luickx, N., Dubruel, P., Van Vlierberghe, S., & De Belie, N.
175 (2015b). pH-responsive superabsorbent polymers: A pathway to self-healing of mortar. *Reactive and*
176 *Functional Polymers*, 93(0), 68-76.

177 Mohammad J. Zohuriaan-Mehr, K. K. (2008). Superabsorbent Polymer Materials: A Review. *Iranian*
178 *Polymer Journal*, 17((6)), 451-477.

179 Nesrinne, S., & Djamel, A. (2013). Synthesis, characterization and rheological behavior of pH sensitive
180 poly(acrylamide-co-acrylic acid) hydrogels. *Arabian Journal of Chemistry*(0).

181 Pourjavadi, A., Barzegar, S., & Zeidabadi, F. (2007). Synthesis and properties of biodegradable
182 hydrogels of κ-carrageenan grafted acrylic acid-co-2-acrylamido-2-methylpropanesulfonic acid as
183 candidates for drug delivery systems. *Reactive and Functional Polymers*, 67(7), 644-654.

184 Povh, B., & Rosina, M. (2005). *Scattering and structures: essentials and analogies in quantum physics*.
185 Springer Science & Business Media.

186 Snoeck, D. (2015). Self-healing and microstructure of cementitious materials with microfibres and
187 superabsorbent polymers. Ghent University.

188 Snoeck, D., Schaubroeck, D., Dubruel, P., & De Belie, N. (2014). Effect of high amounts of
189 superabsorbent polymers and additional water on the workability, microstructure and strength of
190 mortars with a water-to-cement ratio of 0.50. *Construction and Building Materials*, 72(0), 148-157.

191 Snoeck, D., Steuperaert, S., Van Tittelboom, K., Dubruel, P., & De Belie, N. (2012). Visualization of
192 water penetration in cementitious materials with superabsorbent polymers by means of neutron
193 radiography. *Cement and Concrete Research*, 42(8), 1113-1121.

194 Snoeck, D., Van Tittelboom, K., De Belie, N., Steuperaert, S., & Dubruel, P. (2012). The use of
195 superabsorbent polymers as a crack sealing and crack healing mechanism in cementitious materials.
196 *Concrete Repair, Rehabilitation and Retrofitting III: 3rd International Conference on Concrete Repair,*
197 *Rehabilitation and Retrofitting, ICCRRR-3, 3-5 September 2012, Cape Town, South Africa* (p. 58): CRC
198 Press.

199 Snoeck, D., Van Tittelboom, K., Steuperaert, S., Dubruel, P., & De Belie, N. (2014). Self-healing
200 cementitious materials by the combination of microfibres and superabsorbent polymers. *Journal of*
201 *Intelligent Material Systems and Structures*, 25(1), 13-24.

202 Viktor Mechtcherine, L. D., Joachim Schulze. (2006). Internal curing by super absorbent polymers
203 (SAP) – effects on material properties of self-compacting fibre-reinforced high performance concrete.
204 In P. L. O. M. Jensen, K. Kovler (Ed.) (pp. 87 - 96): RILEM Publications SARL.

205 Yu, X.-l., Liu, X.-h., Xia, Z.-r., Cheng, D.-b., Xiao, S., Hu, Z.-j., & Yu, X.-m. (2011). Synthesis and Water-
206 retention Property of the PAA-AM-AMPS and PAA-AM Superabsorbent Polymer. *Fine Chemicals*, 5,
207 004.

208 Zhang, B., Cui, Y., Yin, G., Li, X., Liao, L., & Cai, X. (2011). Synthesis and swelling properties of protein-
209 poly(acrylic acid-co-acrylamide) superabsorbent composite. *Polymer Composites*, 32(5), 683-691.

210 Zhou, X., Weng, L., Chen, Q., Zhang, J., Shen, D., Li, Z., Shao, M., & Xu, J. (2003). Investigation of pH
211 sensitivity of poly(acrylic acid-co-acrylamide) hydrogel. *Polymer International*, 52(7), 1153-1157.

212

213